321/Qd370qD 爆炸焊接界面渗碳体的微观结构

王宇飞[1]，　张金民[2]，　岳宗洪[2]，　周　浩[2]，　韩顺昌[2]，　宋　琳[3]

（1. 河南科技大学 材料科学与工程学院，河南 洛阳　471003；
2. 洛阳船舶材料研究所，河南 洛阳　471039；3. 机械工业第四设计院，河南 洛阳　471039）

摘　要：利用透射电镜研究了 321/Qd370qD 爆炸焊接界面附近渗碳体的微观结构. 结果表明，321/Qd370qD 爆炸焊接界面奥氏体侧存在大量渗碳体，近界面处的渗碳体内存在大量亚片层，尺寸约几个纳米. 这些亚片层相互平行，有的亚片层团互相交叉大约呈 70.5°，亚片层团之间符合一定的晶体学取向关系，即相互之间满足绕[110]。方向旋转 180°后或者绕[002]。方向旋转 180°后相重合. 如果在一个亚片层团的附近按上述关系生长出新的亚片层团，则其更容易形核与长大，且受阻力最小. 相邻亚片层的晶体学取向关系可以推测应用到相邻珠光体团上，相邻珠光体团可能存在以上关系.

关键词：爆炸焊接；渗碳体；透射电镜；珠光体

中图分类号：TG456.6　　文献标识码：A　　文章编号：0253－360X(2009)10－0086－03

王宇飞

0　序　　言

在近代电子显微镜应用之前，人们对于珠光体组织的研究，多局限于珠光体团的大小及珠光体片的大小的研究，更微观的研究没有进行. 借助电子显微镜，已有报道共析渗碳体内存在条纹衬度、位错亚结构、台阶结构、条片状衬度等[1]. 近年来，有人对钢中共析渗碳体微观结构采用透射电镜研究发现，共析渗碳体内存在按一定取向分布的相互平行的亚片层，这些亚片层是在渗碳体和铁素体生长的协调性较低及两相交替生长条件下形成的铁素体[2]. 文献[3]认为厚度大于 0.1 μm 的渗碳体内，与长度方向成一定角度的平行、等距条纹不是水纹花样，而是渗碳体以片层堆垛方式生长留下的痕迹，厚度小于 0.1 μm 的渗碳体内衬度均匀，无条纹衬度和其它衬度. 文献[4]报道了利用原子力显微镜技术显示出珠光体中渗碳体中的双层精细结构和铁素体的细小颗粒. 珠光体中渗碳体和铁素体的取向关系分别存在 Pitsch-Petch，Bagaryatsky，Isaichev 关系. 对相邻珠光体晶体学取向未见报道. 研究渗碳体的微观结构对于珠光体相变的研究具有重要意义. 文中研究了 321/Qd370qD 爆炸焊接界面处渗碳体的微观结构.

收稿日期：2008－07－15

1　试验方法

爆炸焊接所用复板为 321 奥氏体不锈钢，基板为桥梁钢 Qd370qD。从成品上线切割下 0.5 mm 薄片后，在金相砂纸上将其磨到 50 μm，随后用 5%高氯酸酒精电解液，双喷电解抛光，再用氩离子减薄，制得 TEM 样品. 用 CM200 透射电镜观察其微观组织特征.

2　试验结果与分析

爆炸焊接基板组织为珠光体＋铁素体，复板为奥氏体，焊接界面为准正弦波形. 通过透射电镜观察，在距离界面非晶约 200 μm 复板侧，存在一些长条状渗碳体，如图 1a 所示，此处奥氏体大多已经转变为铁素体. 较多渗碳体沿原奥氏体晶界析出，长约几微米，如图 1b 所示. 再往界面方向，渗碳体平行排列，变得较为细长，且数量较多，已经显示出珠光体组织特征，如图 1c 所示. 继续往界面方向，渗碳体占据绝大部分，衬度完全由平行排列的片层和互相交叉在一起的片层组成. 渗碳体内存在的亚片层，深色和浅色平行排列，片层宽度不等，大小约几纳米，亚片层是渗碳体（深色）和铁素体（浅色），如图 1d，e 所示. 因此，此区域也可以叫做珠光体，这么细的亚片层结构还很少有报道. 通常珠光体可分为屈氏体、索氏体和珠光体，其片层宽度分别为 100

~150 nm，250~300 nm，600~1 000 nm. 片层只有几纳米，可能是一种特殊的珠光体. 这种珠光体的形成可能是在高温时发生了共析转变，先形成了极细的亚片层，经过急速冷却保留了下来. 文献[5]认为，在 Fe-C 二元合金中片状珠光体生长是相互协调的，铁素体和渗碳体的生长速率基本相同，如果有第三组元的参与及再分配，则会影响两个新相的生长速度，破坏生长的协调程度. 因而在一个渗碳体方向上会有铁素体和渗碳体亚片层的交替出现. 文中爆炸焊接界面处有 Cr，Mn 等元素，这些元素的参与及再分配，促使渗碳体内渗碳体亚片层和铁素体亚片层的交替生长. 图 1d 中间的条纹衬度与图 1e 明显不同，条纹间距相等，衬度黑白分明，这是渗碳体与铁素体之间由于二次衍射产生的水纹图，即莫尔条纹(如图中箭头处所示).

图 1e有两种方向的亚片层，相互交织在一起，

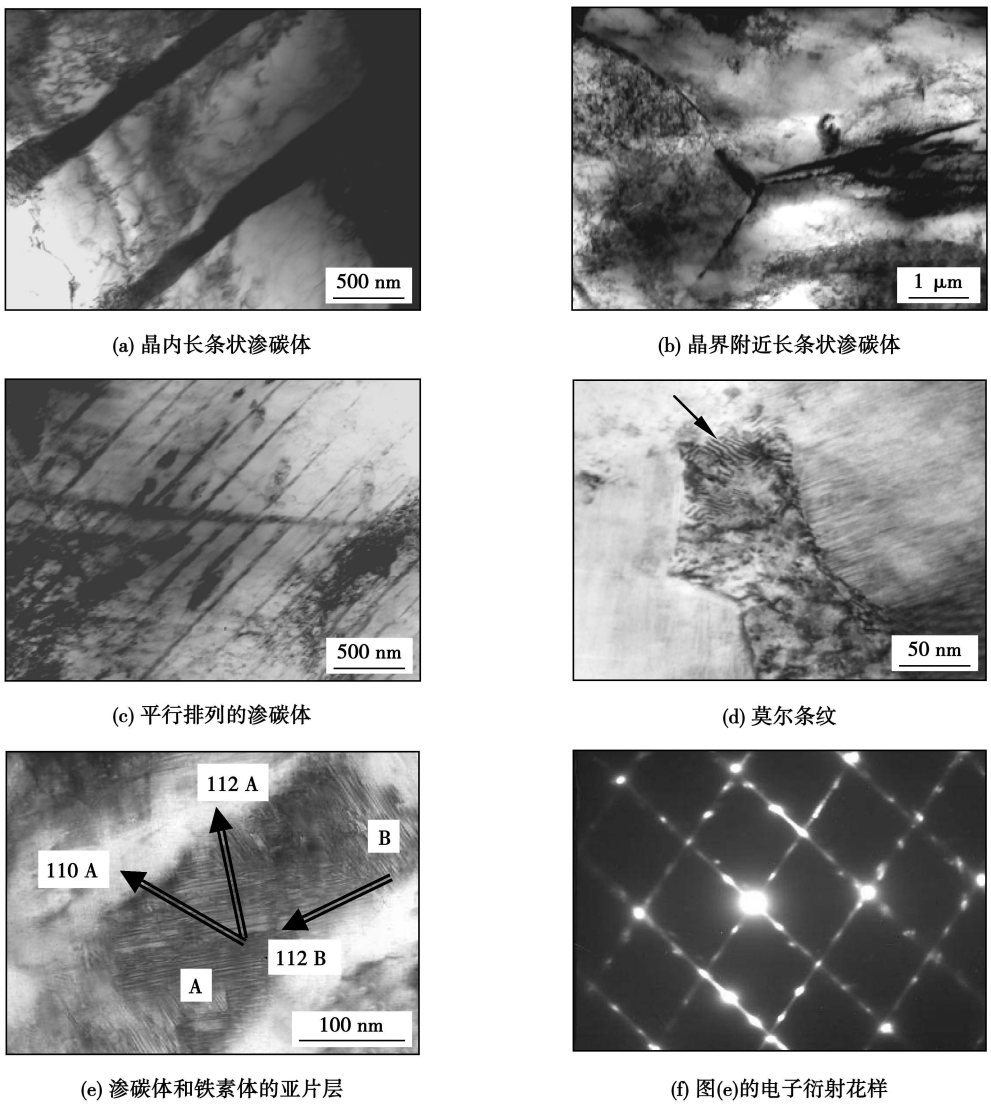

(a) 晶内长条状渗碳体　(b) 晶界附近长条状渗碳体

(c) 平行排列的渗碳体　(d) 莫尔条纹

(e) 渗碳体和铁素体的亚片层　(f) 图(e)的电子衍射花样

图 1　渗碳体透射电镜照片

Fig 1　TEM photos of cementite

呈草丛状，两种方向之间的夹角约呈 70.5°. 图 1f 是图 1e 的电子衍射花样，其电子衍射花样呈条纹状，这是层状结构的倒易点特征，其条纹方向应该与层状形貌垂直. 可以得出渗碳体和铁素体的亚片层平面为(112)$_\alpha$，或者是(001)$_C$. 从图 1e 和电子衍射图可以看出，图中 A 区沿[002]$_\alpha$ 方向旋转 180°后或者 A 区沿[110]$_\alpha$ 方向旋转 180°后，片层方向与 B 区一致，与电子衍射图相吻合. 可见，亚片层团之间符合一定的晶体学取向关系，即相互之间满足绕[110]$_\alpha$ 方向旋转 180°后或者绕[002]$_\alpha$ 方向旋转 180°后相重合(图 2).

图 2a 是某个亚片层团的电子衍射花样，其铁素体的[$\bar{1}$10] 晶带轴与渗碳体的[100] 晶带轴相互平行. 图 2b 是与图 2a 相邻亚片层团的电子衍射花

样,其铁素体的[1$\bar{1}$0] 晶带轴与渗碳体的[$\bar{1}$00] 晶带轴相互平行. 图 2a 沿[110]$_\alpha$ 旋转 180°后与图 2b 电子衍射花样相同,图 2a 与图 2b 的复合得到图 2c 的复合电子衍射花样(对应图 1f). 这样的晶体学关系使相邻亚片层团共用铁素体的(002),(110),(112)面,共用了渗碳体的(006)面,如果在一个亚片层团的附近生长出新的亚片层团,则其更容易形核与长大,且受阻力最小;因此,这种亚片层团与形核母相存在一定的晶体学取向关系. 这种亚片层团的形成机制与珠光体的形成机制类似,相邻亚片层的晶体学取向关系可以推测应用到相邻珠光体团上,相邻珠光体团可能存在以上关系.

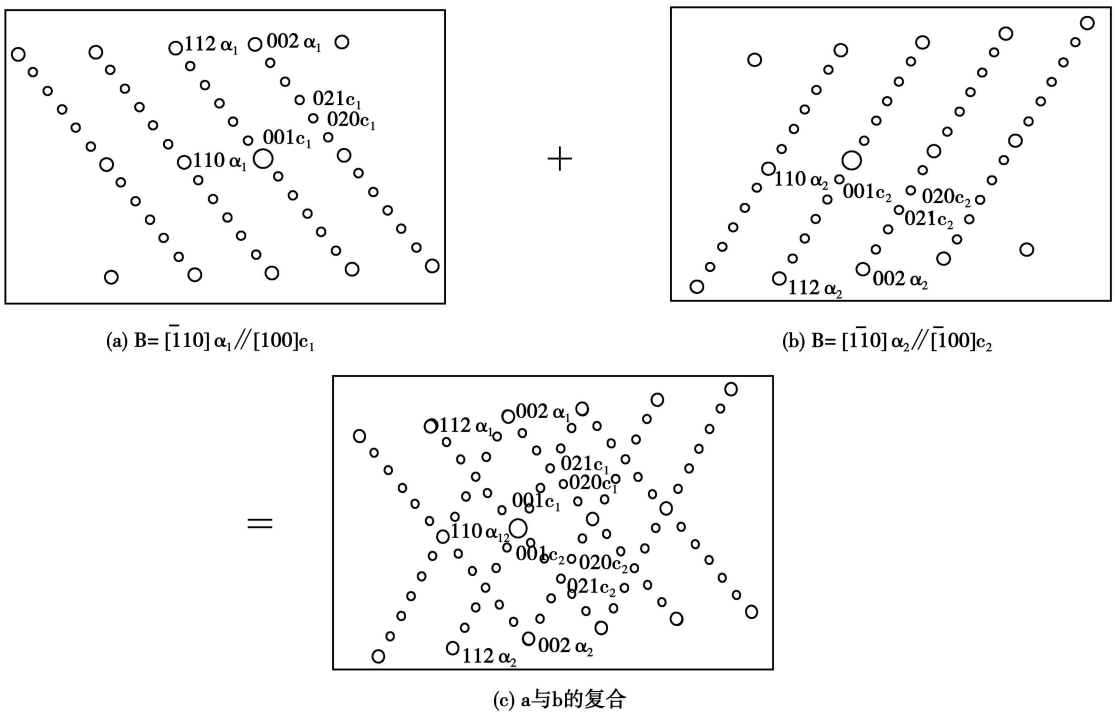

(a) B= [$\bar{1}$10] α_1 // [100]c_1

(b) B= [1$\bar{1}$0] α_2 // [$\bar{1}$00]c_2

(c) a与b的复合

图 2 对应图 1f 电子衍射花样的形成示意图

Fig. 2 Electron diffraction pattern formation schematic of Fig. 1f

3 结 论

321 钢(Qd370qD)爆炸焊接界面奥氏体侧存在大量渗碳体,靠近界面处的渗碳体内存在大量亚片层,其尺寸约几个纳米. 这些亚片层相互平行,有的亚片层团互相交叉,大约呈 70.5°,亚片层团之间符合一定的晶体学取向关系,即相互之间满足绕[110]$_\alpha$ 方向旋转 180°后或者绕[002]$_\alpha$ 方向旋转 180°后相重合. 这样,如果在一个亚片层团附近生长出新的亚片层团,则其更容易形核与长大,且受阻力最小.

参考文献:

[1] 黄孝瑛, 郭 薇, 潘天喜, 等. 珠光体钢微观结构和断裂过程的TEM 研究[J]. 金属学报, 1987, 23(3): 37—41.
Huang Xiaoying, Guo Wei, Pan Tianxi, *et al*. TEM investigation on microstructure and fracture proces of a pearlitic steel[J]. Acta Metallurgica Sinica, 1987, 23(3): 37—41.

[2] 郭正洪. 钢中珠光体相变机制的研究进展[J]. 材料热处理学报, 2003, 24(3): 1—7.
Guo Zhenghong. Progress in the pearlitic transformation mechanism in steels[J]. Transactions of Materials and Heat Treatment, 2003, 24(3): 1—7.

[3] 黄新民. 共析渗碳体结构与变形行为的透射电镜研究[J]. 钢铁研究学报, 2000, 12(2): 60—62.
Huang Xinmin. TEM investigation on the microstructure and deformation behavior of eutectoid cementite[J]. Journal of Iron and Steel Research, 2000, 12(2): 60—62.

[4] 王军艺, 肖新星, 李 健. 测定珠光体片层间距的原子力显微镜技术[J]. 宝钢技术, 2006(6): 36—38.
Wang Junyi, Xiao Xinxing, Li Jian. Atomic force microscope technology for measurement of thickness of lamella pearlite[J]. Baosteel Technology, 2006(6): 36—38.

[5] 朱晓东, 李承基, 章守华, 等. 高碳低合金钢中共析渗碳体微观结构的 TEM 研究[J]. 金属学报, 1998, 34(1): 31—38.
Zhu Xiaodong, Li Chengji, Zhang Shouhua, *et al*. TEM investigation on microstructures of eutectoid cementite in high carbon low alloy steels[J]. Acta Metallurgica Sinica, 1998, 34(1): 31—38.

作者简介: 王宇飞, 男, 1977 年出生, 硕士, 助理教师. 主要从事金属材料理论教学及试验研究. 发表论文 4 篇.

Email: wangyufei05@sina.com

and the weld metal is macroscopically separated into one Fe-rich part and one Cu-rich part. Fe-rich phase is filled in the welding line. At the same time, tensile strength of the welded joint is up to 520 MPa, impact toughness is 32.1 J/cm^2, and surface hardness is also close to HB360, which indicates this technology can meet the need of repair of metal parts in field.

Key words: manual self-propagating high-temperature synthesis welding; material; structure; property

Ultrasonic testing of spot weld based on spectrum analysis and artificial neural network CHEN Zhenhua[1], SHI Yaowu[1], ZHAO Haiyan[2] (1. School of Materials Science and Engineering, Beijing University of Technology, Beijing 100022, China; 2. Department of Mechanical Engineering Tsinghua University, Beijing 100084, China). p 76—80

Abstract: The spectrum of testing signal for the spot weld test is analyzed and the characteristic vector which can indicate the characteristics of the signal spectrum of ultrasonic signals for spot weld is obtained. Through using the vector as input data, an artificial neural network is proposed to classify the resistance spot welds in the different diameter level. The testing method proposed in the paper has the advantages of higher recognition ability, higher efficiency and smaller interference factors compared to the traditional methods.

Key words: resistance spot weld; ultrasonic testing; artificial neural network; characteristic vector

Effect of arc atmosphere on interaction of CO_2 laser beam and TIG arc WU Shikai, XIAO Rongshi, ZHANG Huanzhen (Institute of Laser Engineering, Beijing University of Technology, Beijing 100022, China). p 81—85

Abstract: Laser-arc hybrid welding process is closely related to the arc atmosphere. By using a laser power meter, a beam quality diagnosis instrument and a high speed camera, the beam and arc characteristics were investigated during the vertical interaction between a CO_2 laser beam and a TIG arc in argon and helium atmosphere comparatively. The experimental results demonstrate that the laser power attenuates dramatically, the beam defocuses and the beam quality is seriously worsened while the arc voltage drops, the arc column expands, and even combustion wave supported by a laser generates in argon atmosphere. However, the beam and arc characteristics seldom change during the laser-arc interaction in helium atmosphere. The difference of the laser-arc interaction results from the great difference of the electrons number density due to the difference of the gas ionization energy. The electrons number density in the helium arc is 10 times less than that in the argon arc, and thus the inverse bremsstrahlung absorption coefficient of the helium arc is two orders of magnitude lower than that of the argon arc. Meanwhile, there is less difference of the refractive index between the helium arc and the air, so there is no obvious refraction of the helium arc to the laser beam.

Key words: CO_2 laser; TIG arc; arc atmosphere; inverse bremsstrahlung absorption; refraction

Microstructure of cementite beside interface in 321/Qd370qD explosive welding WANG Yufei[1], ZHANG Jinmin[2], YUE Zonghong[2], ZHOU Hao[2], HAN Shunchang[2], SONG Lin[3] (1. School of Materials Science and Engineering, Henan University of Science and Technology, Luoyang 471003, China; 2. Luoyang Ship Material Research Institute, Luoyang 471039, China; 3. Scivic Engineering Corporation, Luoyang 471039, China). p 86—88

Abstract: Cementite near the interface in 321/Qd370qD explosive welding is analyzed by transmission electron microscopy. The results show that there is a lot of cementite in austenitic side of the interface, and a lot of sub-lamellae exist in the cementite beside the interface. These sub-lamellae are about several nanometers and parallel each other. Some sub-lamella groups cross approximately 70.5° and accord with definite crystal tropism relation, which coincide each other when they circumrotate 180° with $[110]_\alpha$ as axis or with $[002]_\alpha$ as axis. Thus, a new sub-lamella group can easily grow beside another sub-lamella group. The crystal tropism relation of adjacent sub-lamellae may be applied to adjacent pearlite groups that maybe exist the above relation.

Key words: explosive welding; cementite; transmission electron microscopy; pearlite

Corrosion resistance of X80 pipeline steel heat-affected zone in S^{2-} medium BI Zongyue[1,2], Lei Ali[1], WANG Na[1], FENG Lajun[1] (1. School of Materials Science and Engineering, Xi'an University of Technology, Xi'an 710048, China; 2. Baoji Petroleum Steel Pipe Co., Ltd, Shan'xi, Baoji 721008, China). p 89—92

Abstract: A three-electrode electrochemistry method is adopted to research the corrosion resistance of heat-affected zone for X80 pipeline steel welding joint prepared by two welding wires (H06H1 and H05MnNiMo) in the Na_2S solution. The results show that the metallurgical structure of the weld heat-affected zone is needle-like ferrite and granular bainite, and the crystal grain is petty. The corrosion rate of the heat-affected zone increases as the raise of Na_2S concentration and temperature, which the corrosion speed is 0.24—0.81 mm/a when the temperature is 20—60 ℃ and the concentration of Na_2S is 1.0%—2.0%, and the corrosion procedure is the anodic polarization of corrosion system; the corrosion procedure is anodic diffusion when the temperature is above 40 ℃.

Key words: pipeline steel; X80 steel grade; welding heat-affected zone; S^{2-} corrosion

Effects of welding conditions on weld geometry parameters for triple-electrode high-speed CO_2 fillet welding on double sides MA Xiaoli[1], HUA Xueming[1], LIN Hang[1], WU Yixiong[1], Yasuhiko ONIKI[2], Shigeru KAMIFUJI[2], SHI Jiangang[2] (1. Shanghai Key Laboratory of Materials Laser Processing and Modification, Shanghai Jiaotong University, Shanghai 200240, China; 2. Tsuneishi Holdings Corporation, Hiroshima 7200393, Japan). p 93—96